

Coastal Engineering VII, WIT Press, Southampton, pp. 305-311

## **Finite element fault rupture propagation modelling in the Corinth Canal Greece**

F. Gkika, G-A. Tselentis & L. Danciu  
*Seismological Laboratory, University of Patras, Greece*

### **Abstract**

The FEM was used to analyse the pattern of ground deformations caused by the potential slip of a known active fault crossing the Corinth Canal. The analysis was based on detailed geological-Geotechnical data of the area and showed regions possessing high risk of future slope movements and traffic discontinuation across this serious marine navigation project of Eastern Mediterranean.

*Keywords: Rupture propagation, Finite Elements, Corinth Canal, Greece*

### **1 Introduction**

Corinth Canal is 6.3 km long, striking NW-SE and still nowadays is one of the most important marine engineering projects that were made in Greece, Figure 1. Since the opening of the canal in 1893 several problems due to local slope instabilities have been reported. Most of them occur in the Peloponnesus side. The first years of the operation of the canal 14 slides had occurred with total

250.000m<sup>3</sup> of earth material. On the 2<sup>nd</sup> half of the 20<sup>th</sup> century 16 local slope instabilities have been reported in this area.

The main formations that can be seen in the Canal region are Neogene and Quaternary sediments. These are alternating layers of silty marl, marly sandstone, conglomerates and marly limestone intercalated at places by layers of marly clays, silts, sands and gravel. The marly formation dominates in the central horst block of the Corinth Canal and it has been characterized as weak-rock (Andrikopoulou et al [1]).

The Neogene and Quaternary sediments in the canal are cut by numerous sub-vertical faults with nearly East-West striking creating a number of grabens and horsts, (Freyberg [3]). During the latest geotechnical zoning 52 main faults were mapped by Andrikopoulou et al [1]. These faults are crossed by a major system of subvertical joints running parallel to them at an angle 30° to 40° degrees with respect to the Canal axis, (Cristoulas et al [2]).

The strong tectonism of the area supports the qualitative downgrading of the formations especially in the part of the canal where higher and steeper slopes are present. Slopes in the canal exhibit height inclination in the order of 4:1 up to 5:1 and occasionally 6.5:1 and even higher. The maximum slope height is measured ~ 79m above the sea level.

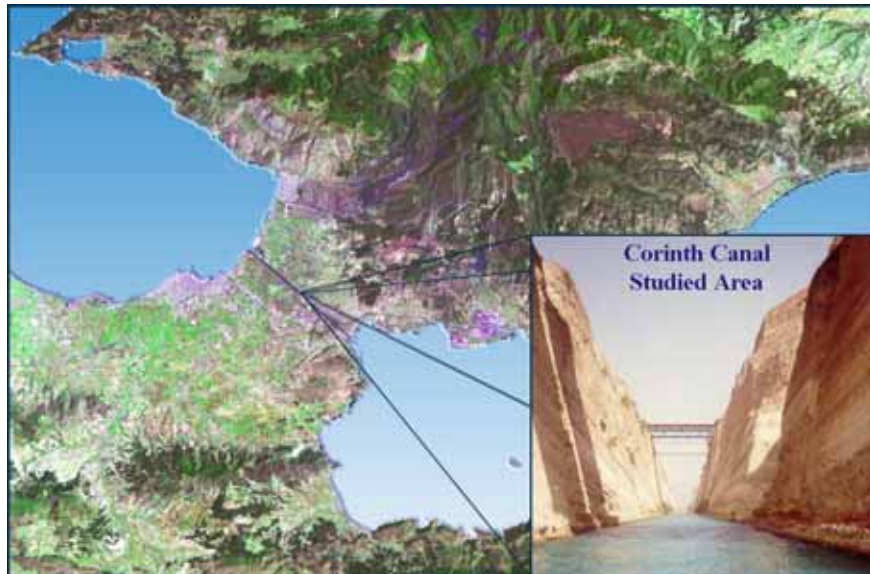


Figure 1: Studied area. A view of the NW border of the canal is also depicted.

The lack of significant run off and the absence of a high unified water table are in favour of the overall stability. Although fault planes are water conduits and slight instability due to erosion and moisture concentration may occur during heavy rain. Fault planes do not contribute by themselves to kinematically unstable conditions nevertheless if they are combined with extensional or stress

relief fissures wedges can be produced, especially at periods with high seismicity, (Andrikopoulou et al [1], Gkika et al [4], Tselentis & Gkika [7]. This is further supported due to the lack of protecting walls for over 4 Km along the canal (wave erosion in the base of the slopes), HCMR [5].

Most of the faults in the canal region are considered active, during earthquake activity moderate to minor surface faulting is been associated with known faults in the canal region. Geodetic investigations in the area revealed that the central part of Corinth Canal appears uplifted relative to the near-coastal areas whereas Possidonia (NW edge of the Canal) shows a trend of subsidence relative to Corinth. The authors believe that the fault reactivation after the 1981 Corinth earthquake sequence was probably associated with small but significant motions detected by geodetic data, (Mariolakos & Stiros [6]).

Considering this problem we simulated fault rupture propagation of a known fault in a part of the Canal where several instability problems have already been reported. The fault that was chosen defines the northern border of the central horst block. It exhibits an E-W direction dipping to the north approximately  $75^\circ$ . According to the geological sections its total displacement is over 10m. The simulation was conducted in order to study the potential damage pattern (deformation distribution) in a local scale and to define a zone of disturbance around the activated fault. In our model we described the complex tectonic geometry that characterizes the area taking into account adjacent major faults. Comparison of the damage distribution in both sides of the canal was additionally conducted (Peloponnesus and Continental Greece).

## **2 Numerical modelling**

### **2.1 General**

Much attention has been devoted in the past to the effects of local soil conditions on seismic ground response and significant progress has been made toward developing analytical models utilizing non-linear inelastic soil behaviour. Very little effort has been devoted, however, to the study of fault rupture propagation through soil and its effects on the pattern of ground deformation in the vicinity of the fault.

In the present investigation the problem was formulated using the FEM and was based on the detailed geological cross section of the canal depicted in Fig.2. The analysis was performed with the finite element program Z-Soil 4.3 which allows non-linear modelling of the behaviour of soil materials in association with a Drucker-Prager failure criterion.

### **2.2 Application**

Simulation of probable activation was implemented for the bounding normal fault on the northern side of the central horst block which is developed on a parallel direction to the Canal axis, (Figure 2). Simulations on both sides of the

canal were conducted using the finite element program Z-Soil 4.3. Due to similarities of the procedure and the results we present mainly the model of the Peloponnesus side. Part of the canal was modeled including the activated fault (site 3300m in Figure 2) with a 500m long and 70m depth finite element mesh that contains over 1370 elements, (Figure 3). The model describes the main geological formations that are present in the studied area (sites 3.050m up to 3.550m) and a number of major faults which are located close to the activated main fault. Non linear behaviour of the geological formations was described using the Drager-Prager failure model.

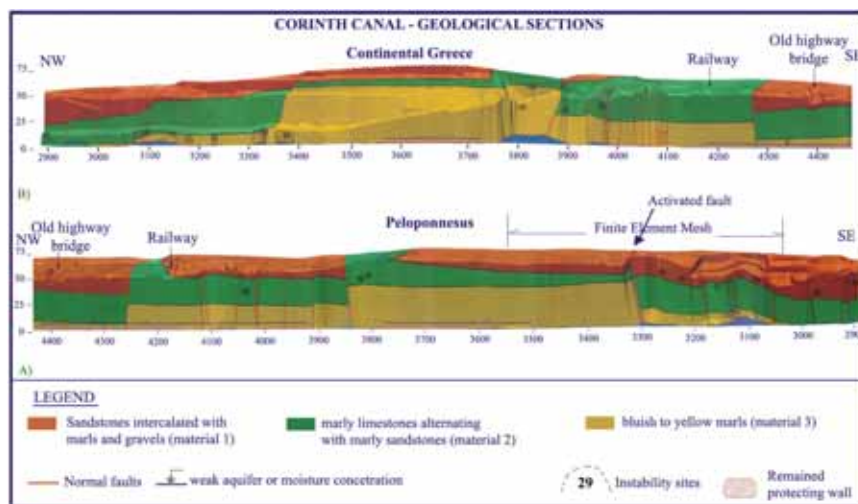


Figure 2: Geological sections of the two sides of the Canal between leveling sites 2+900m and 4+500 m, A) Peloponnesus side, and B) Continental Greece. Triton et al [8].

Figure 2, presents the geological formations in the studying area of the canal plus the sites where instability phenomenon had been reported and the major active faults. As it can be seen in this part of the canal three main geological formations are present. From top to the bottom, sandstones intercalated with marls and gravels (material 1), marly limestones alternating with marly sandstones (material 2) and bluish grey to light yellow marls (material 3), Figure 3 is a finite element model approximation of the studied area.

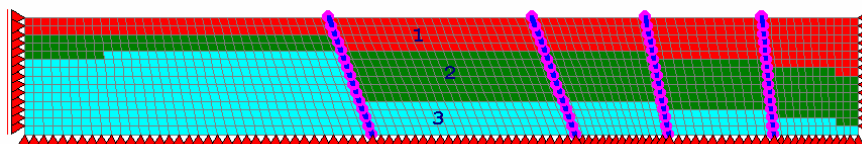


Figure 3: Simplified finite element model describing the main geological formations and major fault close to the activated fault.

Table 1, describes the material properties used to describe the formations that are present in the studied area. These parameters were selected as more representative for the formations by considering the results of several geotechnical investigations that were conducted in the Canal region, (27 offshore & onshore boreholes plus 20 test pits carried out along the base of the canal, 4 boreholes in the region of the new railway construction, 4 older boreholes on the edges of the Canal at Poseidonia & Isthmia sites).

Additionally in the construction area of the new railway the results of two cross-hole investigations were also evaluated.

Table 1: Parameters that were used to describe the geological formations of the Peloponnesus side.

| Parameters | Young modulus<br>E(kPa) | Poisson ratio<br>$\nu$ | Density<br>$\gamma$ (KN/m <sup>3</sup> ) | Cohesion<br>c (kPa) | Friction angle<br>$\phi$ (°) |
|------------|-------------------------|------------------------|--|---------------------|------------------------------|
| Material 1 | 80.000                  | 0.3                    | 20.3                                     | 10                  | 25                           |
| Material 2 | 150.000                 | 0.25                   | 20.6                                     | 182.9               | 53.5                         |
| Material 3 | 250.000                 | 0.25                   | 19.62                                    | 196.25              | 38.8                         |

The analysis procedure can be divided in three basic stages. First, gravity was applied progressively to simulate the time history of the site. This analysis produces “zero displacements and non zero stress” state by superposition of gravity with the stress state produced by gravity. Next, fault slip was simulated by imposing progressively 0.5 m forced displacement on the hanging wall base of the mesh. The forced displacement was imposed in 20 equal steps. Finally stability analysis was implemented resulting to the depicted deformations distribution (total & over the horizontal x-axis), Figures 5 & 6. Additionally, Figure 4 presents the differential settlements calculated over the surface nodes of the finite element mesh.

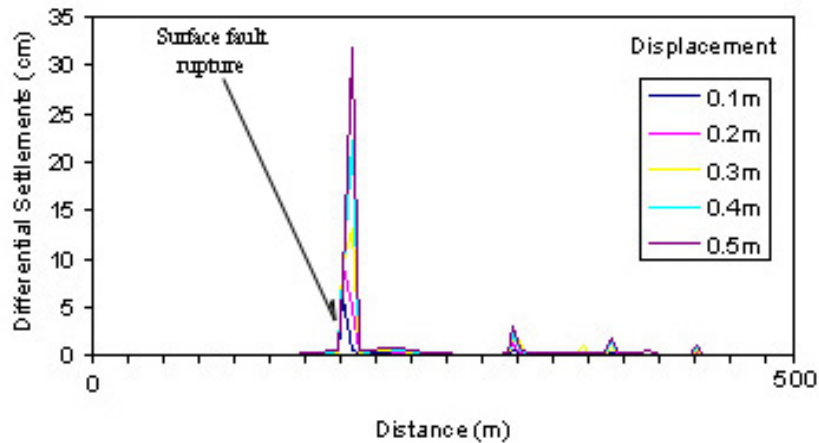


Figure 4: Differential settlements calculated over the surface nodes of the finite element mesh.

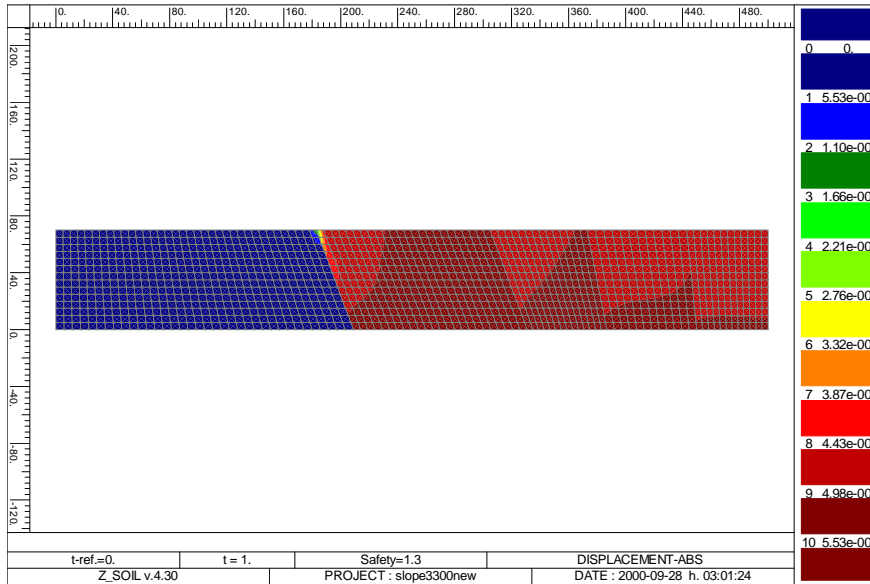


Figure 5: Peloponnesus side, total displacement distributions (m) on every node of the finite element mesh.

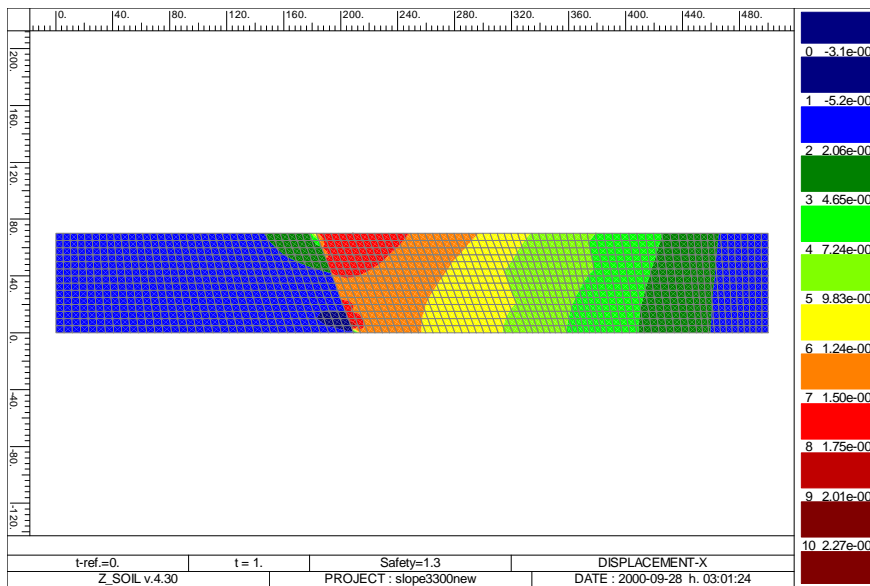


Figure 6: Peloponnesus side, displacement distributions (m) on every node of the finite element mesh over the x-axis (horizontal).

### **3 Conclusions**

Deformation distributions depict a repeated pattern over the tectonic blocks which are defined with the simulated faults. A decrease with distance is depicted with distance from the activated fault and from the base of the finite element mesh to the surface, mainly on the hanging wall. Both sides of the canal present similarities in the deformation distributions due to the similar geometrical pattern of the geological sections.

On the Peloponnesus side damage distribution appears in a wider extent and with higher values of the calculated surface differential settlements. For this reason we have focused our study in this part of the canal. The model that was used for the simulation of potential fault activation does not interpret the creation of new cracks and displacements between adjacent elements. It can be assumed that the calculated maximum displacements will be smaller in potential fault activation.

We define a critical zone of possible instabilities on the Peloponnesus side 200m long in which the higher and wider extent deformations are expected to develop during the potential fault activation. This zone is located between leveling sites 3.350m and 3.150m. Maximum deformations are expected to appear on the surface geological formations at a distance of 50m from the activated fault, on the hanging wall. In this region local instabilities are expected to occur. Finally as it is depicted from Figures 4-6 surface ruptures are expected to appear in the near by faults, too. In this part of the canal a secondary fault reactivation is possible.

Furthermore, wedge type of instabilities and rock falls are more favorable to appear. The problem becomes more severe taking into consideration the continuous erosion due to waves at the base of the canal, the lack of supporting walls and the high seismicity of the region.

### **Acknowledgements**

This work has been partially financed by EC contracts SHIELDS/NNE5/1999/381 & AEGIS IST/2000/26450. One of the authors (F.G.) is grateful to the Greek State Scholarships foundation (I.K.Y.) for financial support. The authors would like to thank Dioriga A.E. and Triton Consulting Engineers for providing useful data from the geotechnical-geophysical investigations in the canal region.

### **References**

- [1] Andrikopoulou K. P., Marinos P. G., Vainalis D., Geotechnical zoning in the Corinth Canal, Engineering Geology of Ancient Works, Monuments and



- Historical Sites, Athens, Greece, Balkema, 1, pp. 231-235, 1988. Becker A.A., The Boundary Element Method in Engineering, McGraw-Hill, New York, 1992.
- [2] Cristoulas S.G., Kalteziotis N.A., Tsiabaos G.K., Geotechnical problems in a bridge over Corinth Canal, Int. Conf. on Case Histories in Geotechnical Engineering, St Louis, Missouri, 3, pp. 849-54, 1984.
  - [3] Freyberg V., Geologie des Isthmus von Korinth, Erlangen Geologische Abhandlungen, 95, pp. 1-183., 1973.
  - [4] Gkika F., Tselentis G-A., Danciu L., Seismic risk assessment of Corinth Canal Greece, Proceedings, 7<sup>th</sup> Internat. Conference on Coastal Engineering, Algarve, Portugal, 2005.
  - [5] HCMR, Hellenic Centre for Marine Research, Special report, Side scan sonar mapping of the Corinth Canal (In Greek), 2001.
  - [6] Mariolakos I., Stiros S. C., Quaternary deformation of the Isthmus and Gulf of Corinthos (Greece), Geology, 15, pp. 225–228, 1987.
  - [7] Triton Consulting Engineers, A.D.K. Consulting Engineers, GAMMA-4 Consulting Geologists – Engineers, Geological mapping in the Corinth Canal between sites 2.900m-4.500m, Peloponnesus and Continental Greece sides, 1999.
  - [8] Tselentis G-A., Gkika F., Boundary element slope instability modelling of Corinth Canal Greece due to nearby fault activation, Proceedings, 7<sup>th</sup> Internat. Conference on Coastal Engineering, Algarve, Portugal, 2005.